Title

Ephrin-as are required for the topographic mapping but not laminar choice of physiologically distinct RGC types

Journal

Developmental Neurobiology, 75(6)

ISSN

1932-8451

Authors

Sweeney, Neal T
James, Kiely N
Sales, Emily C
et al.

Publication Date

2015-06-01

DOI

10.1002/dneu.22265

Peer reviewed

HHS Public Access

Author manuscript

Dev Neurobiol. Author manuscript; available in PMC 2016 June 01.

Published in final edited form as:

Dev Neurobiol. 2015 June ; 75(6): 584–593. doi:10.1002/dneu.22265.

Ephrin-As are required for the topographic mapping but not laminar choice of physiologically distinct RGC types

Neal T. Sweeney, **Kiely N. James**, **Emily Sales**, and **David A. Feldheim**

Molecular, Cell & Developmental Biology, University of California, Santa Cruz, Santa Cruz, CA 95064, USA

Abstract

In the retinocollicular projection, the axons from functionally distinct retinal ganglion cell (RGC) types form synapses in a stereotypical manner along the superficial to deep axis of the SC. Each lamina contains an orderly topographic map of the visual scene but different laminae receive inputs from distinct sets of RGCs, and inputs to each lamina are aligned with the others to integrate parallel streams of visual information. To determine the relationship between laminar organization and topography of physiologically defined RGC types, we used genetic and anatomical axon tracing techniques in wild type and ephrin-A mutant mice. We find that adjacent RGCs of the same physiological type can send axons to both ectopic and normal topographic locations, supporting a penetrance model for ephrin-A independent mapping cues. While the overall laminar organization in the SC is unaffected in ephrin-A2/A5 double mutant mice, analysis of the laminar locations of ectopic terminations shows that the topographic maps of different RGC types are misaligned. These data lend support to the hypothesis that the retinocollicular projection is a superimposition of a number of individual 2-D topographic maps that originate from specific types of RGCs, require ephrin-A signaling, and form independently of the other maps.

Introduction

The mouse superior colliculus (SC) receives input from a number of functionally distinct retinal ganglion cell (RGC) types that form synapses in a stereotypical manner. Along the superficial to deep axis of the mouse SC, inputs from different sets of RGCs are organized into laminae. For example, On-Off direction selective (On-Off DS) RGCs project to the most superficial layer of the SC, while several types of non-DS RGCs project to a slightly deeper SC lamina (Huberman et al., 2008; Huberman et al., 2009; Kay et al., 2011; Kim et al., 2010). Each SC lamina also contains an orderly topographic map of the visual scene, with the Nasal-Temporal (N-T, azimuth) axis of the visual field mapping topographically along the anterior-posterior (A-P) axis, and the dorsal-ventral (D-V, elevation) axis of the visual field mapping topographically along medial-lateral (M-L) axis (reviewed in (Cang and Feldheim, 2013). Thus the retinocollicular projection can be thought of as a superimposition of a number of individual 2-D topographic maps that originate from

Corresponding Author: David A. Feldheim, Professor, Molecular, Cell & Developmental Biology, University of California, Santa Cruz, 1156 High Street, Santa Cruz, CA 95064, phone: 831-459-1797, fax: 831-459-3139, feldheim@biology.ucsc.edu.

Conflict of interest: none

specific types of RGCs, each being aligned with all the others (Figure 1, Dhande and Huberman, 2014)

During embryonic development, RGC axons originating from multiple RGC types enter the SC broadly and then refine to a final topographic and then laminar position (Simon and O'Leary, 1992;Osterhout et al.; Kim et al., 2010). Although much is understood about the mechanisms of topographic mapping, many important questions remain. Among these is the nature of ephrin-A-independent mapping signals. We and others have shown that although some RGC axons from EphA and ephrin-A mutant retinae show defects in topographic mapping along the A-P axis of the SC, a proportion of RGCs still project axons to the correct termination zone (Cang et al., 2008; Pfeiffenberger et al., 2006), even in ephrin-A2/A3/A5 triple knockout mice (Pfeiffenberger et al., 2006;Cang et al., 2008). Two non-mutually exclusive models used to explain these results are: 1) each RGC reads multiple cues and other cues can substitute in the absence of ephrin-As (a penetrance model); or 2) there are distinct ephrin-A dependent and independent RGCs, perhaps representing different functional types (a type-specific model, Feldheim and O'Leary, 2012).

Another unanswered question is whether the individual topographic maps of different RGC types maintain alignment in ephrin-A mutant mice. Although the overall topography is disrupted in ephrin-A mutants, alignment of different RGC types could be maintained, for example if the map of one RGC type serves as a template for other types, as is the case for the mapping of cortical inputs to the SC (Triplett et al., 2009). Alternatively, each RGC type could map topographically independent of the other types, which could lead to misalignment of different RGC maps in ephrin-A mutants. If the different maps maintain alignment with each other, the ectopic termination zones of RGC axons in ephrin-A mutants would be composed of all RGC types; however if ephrin-A mutations cause RGC maps in the SC to lose alignment, ectopic termination zones could include a partial complement of RGC types. As topographic mapping occurs before laminar refinement, another possibility is that topographic defects in ephrin-A mutant mice could affect SC laminar organization. If so, this would suggest either that formation of topography and lamination are coupled events or that both require EphA/ephrin-A signaling.

Here we take advantage of recently described transgenic mice lines that express GFP in functional RGC types that project to specific SC lamina to ask if ephrin-A signaling is involved in RGC subtype mapping. We find that the TZs from RGCs of the same physiological type (or two TZs from the same RGC) can be in both ectopic and normal topographic locations. As we did not find a specific RGC class that was insensitive to the loss of ephrin-A signaling, these results support a penetrance model rather than a type-specific model to explain the correct RGC projections in EphA and ephrin-A mutants. Analysis of the SC laminar locations of ectopic termination zones in ephrin-A5 mutant and ephrin-A2/A5 double mutant mice reveals that RGC topographic maps can be misaligned, suggesting that activity-dependent mechanisms are not sufficient to maintain alignment of all RGC types. Finally, we find that the RGC lamination patterns in the SC are unaffected in ephrin-A2/A5 double mutant mice, indicating that lamination and topography develop using distinct processes.

Methods

Mice

Adult (P20–P30) ephrin-A5 mutant and ephrin-A2/A5 mutant mice were generated and genotyped as previously described (Feldheim et al., 2000). Ephrin-A2 or ephrin-A5 heterozygote mice were used as controls for all experiments. Animals were cared for and used in accordance with guidelines of the U.S. Public Health Service Policy on Humane Care and Use of Laboratory Animals and the NIH Guide for the Care and Use of Laboratory Animals, and following institutional Association for Assessment and Accreditation of Laboratory Animal Care-approved practices.

Axon tracing

Adult (P20–P30) mice were anaesthetized by intraperitoneal injection of 100 mg/kg ketamine and 10 mg/kg xylazine. For RGC labeling, a small amount of 1,1'-dioctadecyl-3,3,3',3'-tetramethylindocarbocyanine (DiI, Invitrogen, Carlsbad,10 % in *N*,*N*-dimethylformamide) was injected using a handheld picospritzer (Parker Instrumentation, Cleveland) and a pulled glass needle at focal regions intraocularly as described previously (Feldheim et al., 2000).

Antibody staining of brain sections and fluorescent microscopy

One week after injection of DiI, animals were sacrificed and intracardially perfused with ice-cold 4% paraformaldehyde (PFA) in PBS. Brains were dissected out and fixed overnight in 4% PFA at 4°C. The following day, brains were washed with PBS and incubated in 30% sucrose at 4°C overnight. 100 μm parasagittal sections were cut with an HM430 sliding microtome (Thermo-Fisher, Waltham, MA, USA). Sections were incubated in blocking buffer (5% goat serum in PBS/0.1% TritonX-100) for one hour at room temperature, then incubated in GFP rabbit polyclonal, at 1:1,000 dilution, in blocking buffer (Life Technologies, Carlsbad, CA, USA) overnight at 4°C with rocking. The following day, sections were washed in PBS at room temperature (3 × 30 minutes) and incubated with fluorescently-conjugated secondary antibodies diluted at 1:1,000 in blocking buffer for 1 hour at room temperature. Sections were washed (3 × 30 minutes) and a coverslip was mounted using Fluoromount-G (Southern Biotechnology, Birmingham, AL, USA). Imaging was performed with an Olympus BX51 epifluorescent microscope (Olympus, Center Valley, PA, USA) equipped with QImaging Retiga EXi digital camera (QImaging, Surrey, BC, Canada).

Retrograde labeling of RGCs

Adult mice were anesthetized using isoflurane and placed in a stereotaxic instrument. After trimming the fur, an incision in the skin was made to expose the skull and a dental drill was used to open the skull. Having attained bilateral access the SC (relative to Bregma: A-P −2.9, M-L ±0.6, D-V −1.3 mm), DiI was injected using a picospritzer. Mice were perfused with 4% PFA 5–6 days after DiI injection. The eyes were removed and the retinas dissected out, postfixed overnight with 4% PFA, and stained for cocaine- and amphetamine-regulated transcript (CART, Phoenix H-003-62, 1:1000) and SMI-32 (Covance SMI-32P, 1:2500).

Retinas were imaged on a Leica DM5500 B widefield microscope using a 10× objective, then on a Leica DMI6000 confocal microscope using a 40× objective and Argon (488) and HeNe (543, 633) lasers to collect confocal Z-stacks at 0.5 μm. Z-stacks and maximal projection images were used to manually count the number of SMI-32+ or CART+ neurons per frame either labeled or unlabeled by DiI, as well as the total number of neurons labeled by DiI.

Statistics

In Figure 3, we calculated the percent of total DiI-labeled RGCs that were co-labeled with either SMI-32 or CART. For normalized measurements, the initial percentages were normalized by dividing them by a normalizing factor n, where n was the total number of SMI-32 (or CART) in the sample image divided by the maximal number of SMI-32 (or CART) present in any sample image. Normalized percentages were compared using a two-way ANOVA followed by Holm-Sidak's multiple comparison's test.

Quantification of fluorescence

Quantification of fluorescence intensity across SC lamina was achieved using the Plot Profile function in ImageJ (National Institutes of Health, Bethesda, MD). A 100 by 100 pixel square was drawn perpendicular to the SC surface and was normalized and binned as in Huberman et al, 2009.

Results

RGCs that project to topographically correct or incorrect locations in ephrin-A mutant mice do not belong to a specific RGC class

To analyze topography and lamination of the retinocollicular projection, we anterogradely traced RGCs using focal injections of DiI in the nasal retina in transgenic mice expressing GFP in RGC subsets. For most of the experiments, we used transgenic mice (TRHR-GFP or DRD4-GFP) that label On-Off DS RGCs that project to the superficial laminae of the SC (upper stratum griseum superficiale or uSGS) (Huberman et al., 2008; Rivlin-Etzion et al., 2011) (Figure 1). After sectioning the SC along the sagittal axis, DiI-labeled axon terminations were visualized using fluorescent microscopy and the lamination location of the termination zone (TZ) identified using the GFP-labeled axons.

In wild-type mice, a focal injection of DiI in the nasal retina reliably produced a topographically correct TZ in the posterior SC (Figure 2A1). In ephrin-A5 mutant mice, 81% of injections produced ectopic TZs at topographically incorrect locations; in addition, all ephrin-A5 mutants we examined (n=74) had a correct TZ (Figure 2B1 and 2C1), as we reported previously (Feldheim et al., 2000). We sectioned the brains and compared the lamination patterns of the correct and ectopic TZs with that of the TRHR-GFP or DRD4-GFP axons that labeled superficial SC laminae and analyzed whether the axons projected only to superficial uSGS laminae, only to deeper uSGS laminae, or to all uSGS laminae. In wild-type mice, we found that in all cases (n=12), the correct TZ projected to all uSGS laminae (Figure 2A2–4). This is consistent with our assumption that a focal injection of DiI in nasal retina labels all RGC types at that location, including those projecting to superficial

and deep uSGS layers. In ephrin-A5 mutant mice, the correct TZ also extended to all uSGS laminae in all mice (n=12), suggesting that these do not represent a particular RGC class or set of classes, and that all RGC types have the capacity to project to the topographically correct location in the absence of ephrin-A5 (Figure 2B4 and 2C4).

In examining the ectopic TZs (n=12) in ephrin-A5 mutant mice, we found that 58% projected to both superficial and deep uSGS laminae (Figure 2B2–4), while the remaining 42% were localized to superficial uSGS laminae (Figure 2C2–4). The ectopic TZs that projected to all layers likely include multiple RGC types that stayed in register despite making mapping errors. The ectopic TZs that only projected to the superficial laminae are likely a cluster of RGCs that lost alignment with other misprojecting RGCs. Interestingly, in ephrin-A5 mutants we did not find ectopic TZs that only projected to the deep laminae.

Different RGC types show different levels of dependence on ephrin-As in topographic mapping

We also wondered if different types of RGCs are equally dependent on EphA/ephrin-A signaling to attain an orderly retinocollicular map. In wild type mice, a collicular injection of DiI labels a cluster of RGC in the retina, the location of which depends on the A-P and D-V coordinates of the collicular injection (Rashid et al., 2005). In ephrin-A5 mutants, such a collicular injection labels both a group of RGCs that are in the topographically correct position as well as some that are spread along the N-T axis of the retina (Figure 3A, 3B). In order to determine if the topographically incorrect RGCs are of a distinct type, we immunostained ephrin-A5 mutant retina with two antibodies that label distinct RGC types: 1) Cocaine- and amphetamine-regulated transcript (CART), which is expressed in On-Off DS RGCs (Kay et al., 2011), and 2) SMI-32, which is expressed in large alpha-RGCs (Lin et al., 2004; Schmidt et al., 2014, but see Coombs, et al., 2006). We found DiI-labeled cells of both RGC types in topographically incorrect as well as topographically correct regions (Figure 3C–F). We also wanted to examine the ephrin-A sensitivity of each RGC type. After normalizing for the number of CART+ or SMI-32+ cells imaged, we found no significant difference in the percent of either CART+/DiI+ RGCs or SMI-32+/DiI+ RGCs found in the topographically correct vs. topographically incorrect locations of the retina, indicating that CART+ RGCs are no more or less sensitive to the loss of ephrin-A2 and -A5 than average for all RGCs (Figure 3C–F and Table 1).

The topographic maps of different RGC types are misaligned in ephrin-A mutant mice

We next wanted to determine if the topographic maps of individual RGC types maintain their alignment when topography is disrupted. Here we used ephrin-A2/A5 double mutants as these have more ectopic TZs than ephrin-A5 single mutant mice (Feldheim et al., 2000). We injected DiI into the nasal retina and sectioned the brains to determine the lamination patterns of topographically correct and ectopic TZs in the SC. We found that 96% of ephrin-A2/A5 double knockouts showed ectopic TZs and many of these showed multiple ectopic TZs. As with ephrin-A5 mutants, each A2/A5 double knockout had a correct TZ (n=33) and each of these that we sectioned (n=11) had projections to both the superficial and deep uSGS laminae. For the ectopic TZs (n=24), we found that 46% of these projected to all laminae, 29% were restricted to the superficial laminae and 21% were restricted to the deep laminae.

Figure 4 shows three examples of ectopic TZs and their lamination patterns in ephrin-A2/A5 double mutants. In Figure 4A1–4, three ectopic TZs all projected to the same A-P location of the SC but were out of register along the M-L axis. This is a phenotype we have described previously (Feldheim et al., 2000), although we did not find that these defects lead to altered functional topography along the M-L mapping axis (Cang et al., 2008). Two other examples (Figure 4B1–4 and 4C1–4) show ephrinA2/A5 mutant mice with multiple ectopic TZs that are out of register in the A-P axis, but are only slightly misaligned along the M-L axis. In each case, the columnar distribution of TZs of different RGC types is disrupted such that TZs from the same location in the retina make errors to distinct locations in the SC. For example, in Figure 4C1–4, one ectopic TZ is restricted to the superficial laminae, while another ectopic TZ is restricted to the deep laminae. This suggests that RGCs of different types fail to maintain alignment when in topographically incorrect locations.

Lamination of RGC inputs is preserved in ephrin-A mutant mice

In order to determine if the mechanisms of topographic mapping and laminar formation in the SC are distinct processes, we assessed the laminar location of RGC axons in the TRHR-GFP and DRD4-GFP transgenic mice described above as well as the CB2-GFP mouse line, a line that labels Off-transient RGCs that project axons to deeper laminae of the uSGS (Huberman et al., 2008; Huberman et al., 2009; Rivlin-Etzion et al., 2011). We created ephrin-A2/A5 double mutant mice that also harbor the TRHR-GFP, DRD4-GFP or CB2-GFP transgenes and determined if the axons from these transgenes projected to their proper lamina by sectioning the SC of adult mice and immunostaining to detect GFP in the RGC axons. We find that in ephrin-A2/A5 double mutant mice the axons in each of these GFP lines maintain laminar-specific projections (Figure 5A–B, D–E, G–H). We quantified the amount of GFP fluorescence across the retinorecipient layer of the SC (Figure 5C, 5F, 5I) and did not find any significant differences in normalized intensity between controls and ephrin-A2/A5 mutants. This shows that at least for some RGC types, distinct mechanisms control topographic mapping and lamination.

Discussion

The importance of EphA/ephrin-A signaling in the formation of a topographic map between the N-T axis of the retina and the A-P axis of the superior colliculus is well established. Although some RGC axons make mapping errors in the SC of ephrin-A (Feldheim et al., 2000; Frisén et al., 1998; Pfeiffenberger et al., 2006) and EphA mutant mice (Feldheim et al., 2004; Rashid et al., 2005), some RGCs axons in these mice terminate in the topographically correct locations (Cang et al., 2008). This raises the possibility that there are EphA- and ephrin-A-independent mapping mechanisms that are redundant or can compensate for loss of these signaling molecules. EphA/ephrin-A-independent mechanisms could be used by all RGC types, such that each individual RGC, regardless of type, has the possibility to use these mechanisms (a penetrance model), or by select RGC types, such that some RGCs use EphA/ephrin-A signaling while others do not (a type-specific model). Previous studies were unable to distinguish between these possibilities because of the limitations of anatomical tracing experiments used to assess topographic maps. Here we assayed the topographic maps using anatomical tracing in ephrin-A mutant mice that also

express GFP in a specific RGC type that projects axons to either the superficial or deep laminae of the retinorecipient area of the SC.

Ephrin-A-dependent and -independent topographic mapping in the superior colliculus

In order to test if RGCs of different types require ephrin-As for topographic mapping we created ephrin-A5 single mutant mice and ephrin-A2/A5 double mutant mice that also harbored a GFP-transgene that is expressed in one type of On-Off DS RGCs. Focal DiI injections into these mice show that topographically correct and incorrect terminations both contain RGC axons that project to the same deep laminae as Off-Transient RGCs (labeled by the CB2-GFP transgene) and to the same superficial laminae as On-Off DS RGCs (labeled by the DRD4-GFP or THRH-GFP transgene, Figure 2). It should be noted that our experiments cannot determine if a single RGC can make both correct and ectopic TZs. These results support a penetrance model in which all RGC types require ephrin-As for topographic mapping but in some cases utilize alternative mechanisms to terminate in the appropriate location. Our analysis of retrograde labeling also shows that both RGCs that express CART (an On-Off DS RGC marker) or SMI-32 (an alpha On or Off RGC marker) can project to the either the topographically correct or incorrect position (Figure 3). Neither RGC type that we examined showed a difference in sensitivity to ephrin-As compared to RGCs as a population.

One limitation of this study is that we do not have markers that can differentiate the ~15 different RGC types that project to the SC and therefore we cannot conclude whether there are specific RGC type(s) that are strictly ephrin-A dependent or independent. In addition, here we inferred RGC class based on lamination patterns (superficial vs. deep) but we know that multiple RGC types project to the superficial and deep laminae of the uSGS (Kim et al., 2010). The ongoing development of transgenic mouse lines and molecular markers that label specific RGC types will allow us to assay ephrin-A function more comprehensively.

Alignment of topographic maps of different RGC types in ephrin-A mutant mice

Because RGCs of different types project to different lamina within the SC, one can think of retinocollicular projection not as a single retinotopic map but instead as a superimposition of a number of individual 2-D topographic maps that originate from specific types of RGCs, each being aligned with all the others. Focal DiI injections in the retina label multiple RGC types that target the same A-P and M-L position in the SC, but can project to different SC laminae. For example, several On-Off DS RGC types project to superficial laminae within the retinorecipient area (uSGS), while several non-DS On and Off types project to deeper laminae. When viewed as a parasagittal section, labeled RGCs create a column of DiI label in the SC.

In ephrin-A2/A5 double mutants, we find ectopic termination zones that are laminar-specific, which suggests that columnar alignment is disrupted. We interpret this to mean that activity-dependent mechanisms – in the absence of EphA/ephrin-A signaling – are unable to maintain alignment of different RGC types that project to distinct SC laminae. This result is somewhat inconsistent with a recent report in which receptive field properties SC neurons were analyzed in ephrin-A2/A5 double mutant mice (Liu et al., 2014). The authors found

that although many of the receptive fields of SC neurons were located in topographically inappropriate regions, the On and Off receptive fields of these neurons overlapped. Since it is assumed that SC neurons are innervated by both On and Off RGCs, this suggests that the On and Off RGC maps maintain alignment in ephrin-A2/A5 mutant mice despite receiving inputs from RGCs at topographically incorrect locations. In our experiments, we were not able to determine the types of RGCs being labeled by DiI, but only that some terminate in superficial and some in deeper laminae. It is possible that some RGC types, perhaps those that terminate in the same lamina can maintain alignment when topography is disrupted, while others that are in different lamina may not, perhaps due to selective adhesion between axons of specific sets of RGCs or to differences in the correlated activity patterns between RGC types during development as has been observed for On and Off RGC types in glutamatergic retinal waves in vitro (Kerschensteiner and Wong, 2008).

Lamination of RGC inputs in the superior colliculus

A final question was whether disruption of topography affects SC laminar organization. Different models for SC laminar formation have been proposed. In zebrafish RGC axons picks a precise layer in the tectum (analogous to the SC) early in development in a process that involves Slit-Robo signaling (Xiao et al., 2011), while in mice RGC axons initially project to multiple SC layers before refining (reviewed in (Huberman et al., 2010). In Math5 mutant mice in which only 5–10% of the normal amounts of RGCs persist, the remaining RGC axons project to the superficial SC laminae (Triplett et al., 2011), suggesting that SC lamination is subject to the influence of molecular gradients or axon-axon competition. Here we show that in ephrin-A2/A5 double mutants with disrupted topography, Off-transient and DS RGCs project axons to the normal laminar location, demonstrating that laminar formation utilizes distinct mechanisms from topographic mapping at least for these two distinct cell types.

Acknowledgements

We thank Jena Yamada for technical support. This work was supported by grants from the NIH (R01EY022117 to DAF) and the Glaucoma Research Foundation (DAF), two CIRM Postdoctoral Scholar Training Fellowships (TG2-01157 to NTS) and (TG2-01157 to KNJ), an award from the Initiative for Maximizing Student Diversity (IMSD) at UCSC (ES), and a CIRM Major Facilities Grant (FA1-00617-1 to UCSC).

References

Cang J, Feldheim DA. Developmental mechanisms of topographic map formation and alignment. Annu Rev Neurosci. 2013; 36:51–77. [PubMed: 23642132]

Cang J, Wang L, Stryker MP, Feldheim DA. Roles of ephrin-as and structured activity in the development of functional maps in the superior colliculus. J Neurosci. 2008; 28:11015–11023. [PubMed: 18945909]

Dhande OS, Huberman AD. Retinal ganglion cell maps in the brain: implications for visual processing. Curr Opin Neurobiol. 2014; 24:133–142. [PubMed: 24492089]

Feldheim DA, Kim YI, Bergemann AD, Frisen J, Barbacid M, Flanagan JG. Genetic analysis of ephrin-A2 and ephrin-A5 shows their requirement in multiple aspects of retinocollicular mapping. Neuron. 2000; 25:563–574. [PubMed: 10774725]

Feldheim DA, Nakamoto M, Osterfield M, Gale NW, DeChiara TM, Rohatgi R, Yancopoulos GD, Flanagan JG. Loss-of-function analysis of EphA receptors in retinotectal mapping. J Neurosci. 2004; 24:2542–2550. [PubMed: 15014130]

Feldheim DA, O'Leary DD. Visual map development: bidirectional signaling, bifunctional guidance molecules, and competition. Cold Spring Harb Perspect Biol. 2012; 2:a001768. [PubMed: 20880989]

Frisén J, Yates PA, McLaughlin T, Friedman GC, O'Leary DDM, Barbacid M. Ephrin-A5 (AL-1/RAGS) is essential for proper retinal axon guidance and topographic mapping in the mammalian visual system. Neuron. 1998; 20:235–243. [PubMed: 9491985]

Huberman AD, Clandinin TR, Baier H. Molecular and cellular mechanisms of lamina-specific axon targeting. Cold Spring Harb Perspect Biol. 2010; 2:a001743. [PubMed: 20300211]

Huberman AD, Manu M, Koch SM, Susman MW, Lutz AB, Ullian EM, Baccus SA, Barres BA. Architecture and activity-mediated refinement of axonal projections from a mosaic of genetically identified retinal ganglion cells. Neuron. 2008; 59:425–438. [PubMed: 18701068]

Huberman AD, Wei W, Elstrott J, Stafford BK, Feller MB, Barres BA. Genetic identification of an On-Off direction-selective retinal ganglion cell subtype reveals a layer-specific subcortical map of posterior motion. Neuron. 2009; 62:327–334. [PubMed: 19447089]

Kay JN, De la Huerta I, Kim IJ, Zhang Y, Yamagata M, Chu MW, Meister M, Sanes JR. Retinal ganglion cells with distinct directional preferences differ in molecular identity, structure, and central projections. J Neurosci. 2011; 31:7753–7762. [PubMed: 21613488]

Kerschensteiner D, Wong RO. A precisely timed asynchronous pattern of ON and OFF retinal ganglion cell activity during propagation of retinal waves. Neuron. 2008; 58:851–858. [PubMed: 18579076]

Kim IJ, Zhang Y, Meister M, Sanes JR. Laminar restriction of retinal ganglion cell dendrites and axons: subtype-specific developmental patterns revealed with transgenic markers. J Neurosci. 2010; 30:1452–1462. [PubMed: 20107072]

Lin B, Wang SW, Masland RH. Retinal ganglion cell type, size, and spacing can be specified independent of homotypic dendritic contacts. Neuron. 2004; 43:475–485. [PubMed: 15312647]

Liu M, Wang L, Cang J. Different roles of axon guidance cues and patterned spontaneous activity in establishing receptive fields in the mouse superior colliculus. Front Neural Circuits. 2014; 8:23. [PubMed: 24723853]

Osterhout JA, El-Danaf RN, Nguyen PL, Huberman AD. Birthdate and outgrowth timing predict cellular mechanisms of axon target matching in the developing visual pathway. Cell Rep. 2014; 8:1006–1017. [PubMed: 25088424]

Pfeiffenberger C, Yamada J, Feldheim DA. Ephrin-As and patterned retinal activity act together in the development of topographic maps in the primary visual system. J Neurosci. 2006; 26:12873–12884. [PubMed: 17167078]

Rashid T, Upton AL, Blentic A, Ciossek T, Knoll B, Thompson ID, Drescher U. Opposing Gradients of Ephrin-As and EphA7 in the Superior Colliculus Are Essential for Topographic Mapping in the Mammalian Visual System. Neuron. 2005; 47:57–69. [PubMed: 15996548]

Rivlin-Etzion M, Zhou K, Wei W, Elstrott J, Nguyen PL, Barres BA, Huberman AD, Feller MB. Transgenic mice reveal unexpected diversity of on-off direction-selective retinal ganglion cell subtypes and brain structures involved in motion processing. J Neurosci. 2011; 31:8760–8769. [PubMed: 21677160]

Schmidt TM, Alam NM, Chen S, Kofuji P, Li W, Prusky GT, Hattar S. A role for melanopsin in alpha retinal ganglion cells and contrast detection. Neuron. 2014; 82:781–788. [PubMed: 24853938]

Simon DK, O'Leary DDM. Development of topographic order in the mammalian retinocollicular projection. J. Neurosci. 1992; 12:1212–1232. [PubMed: 1313491]

Triplett JW, Owens MT, Yamada J, Lemke G, Cang J, Stryker MP, Feldheim DA. Retinal input instructs alignment of visual topographic maps. Cell. 2009; 139:175–185. [PubMed: 19804762]

Triplett JW, Pfeiffenberger C, Yamada J, Stafford BK, Sweeney NT, Litke AM, Sher A, Koulakov AA, Feldheim DA. Competition is a driving force in topographic mapping. Proc Natl Acad Sci U S A. 2011; 108:19060–19065. [PubMed: 22065784]

Xiao T, Staub W, Robles E, Gosse NJ, Cole GJ, Baier H. Assembly of lamina-specific neuronal connections by slit bound to type IV collagen. Cell. 2011; 146:164–176. [PubMed: 21729787]

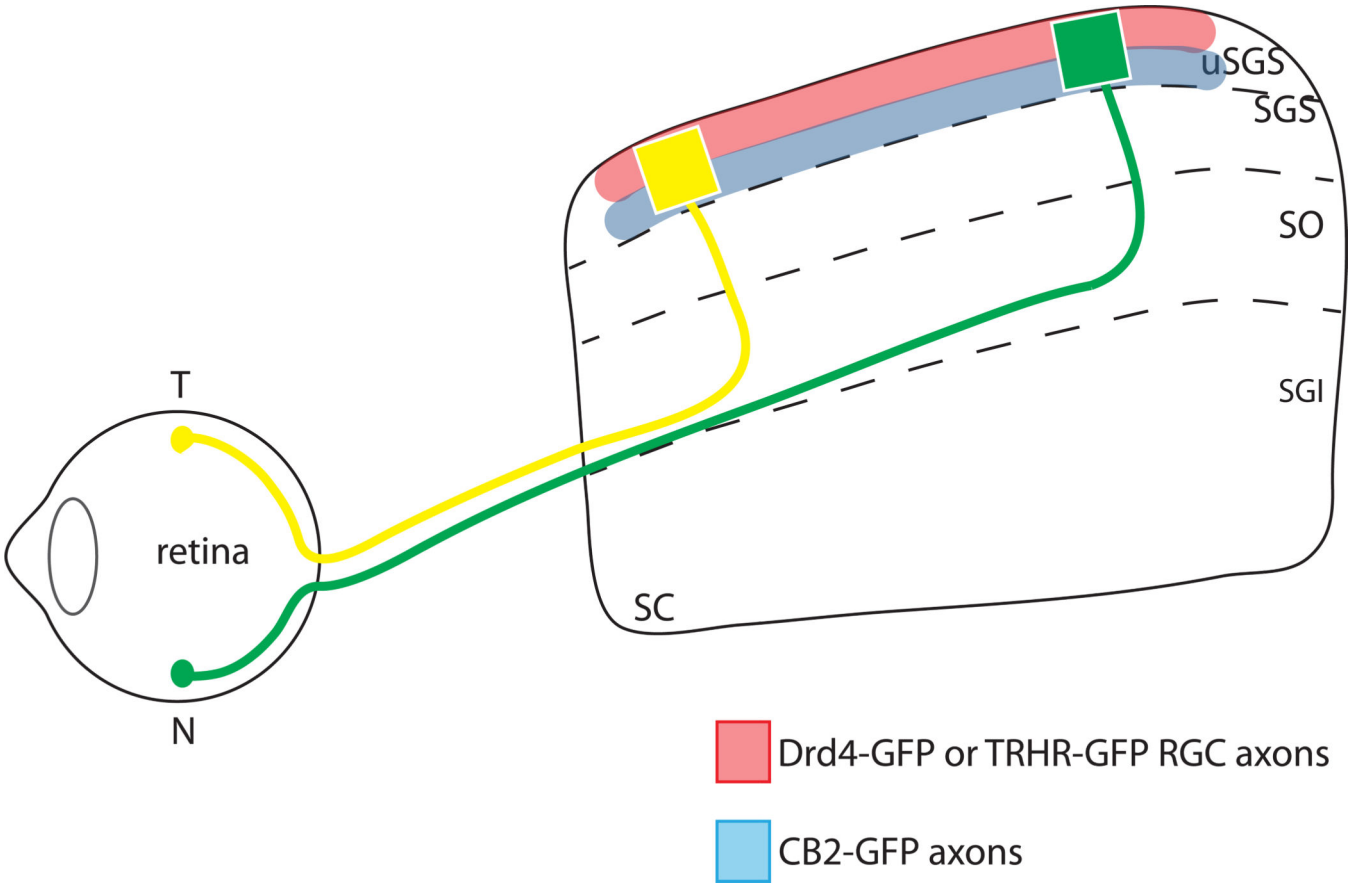

Figure 1. Anterior-posterior topography and lamination patterns of RGC types in the superior colliculus

Temporal (T) axons of all RGC types (yellow) project to the anterior SC and nasal (N) axons (green) project to the posterior SC. Direction-selective RGC types labeled in TRHR-GFP and DRD4-GFP transgenic lines project to superficial laminae of the uSGS (upper stratum griseum superficiale) (red), Off transient RGCs labeled by CB2-GFP transgenic line project to deeper laminae of the uSGS (blue), and different types of RGCs from the same topographic location are aligned along the superficial-deep axis of the SC.

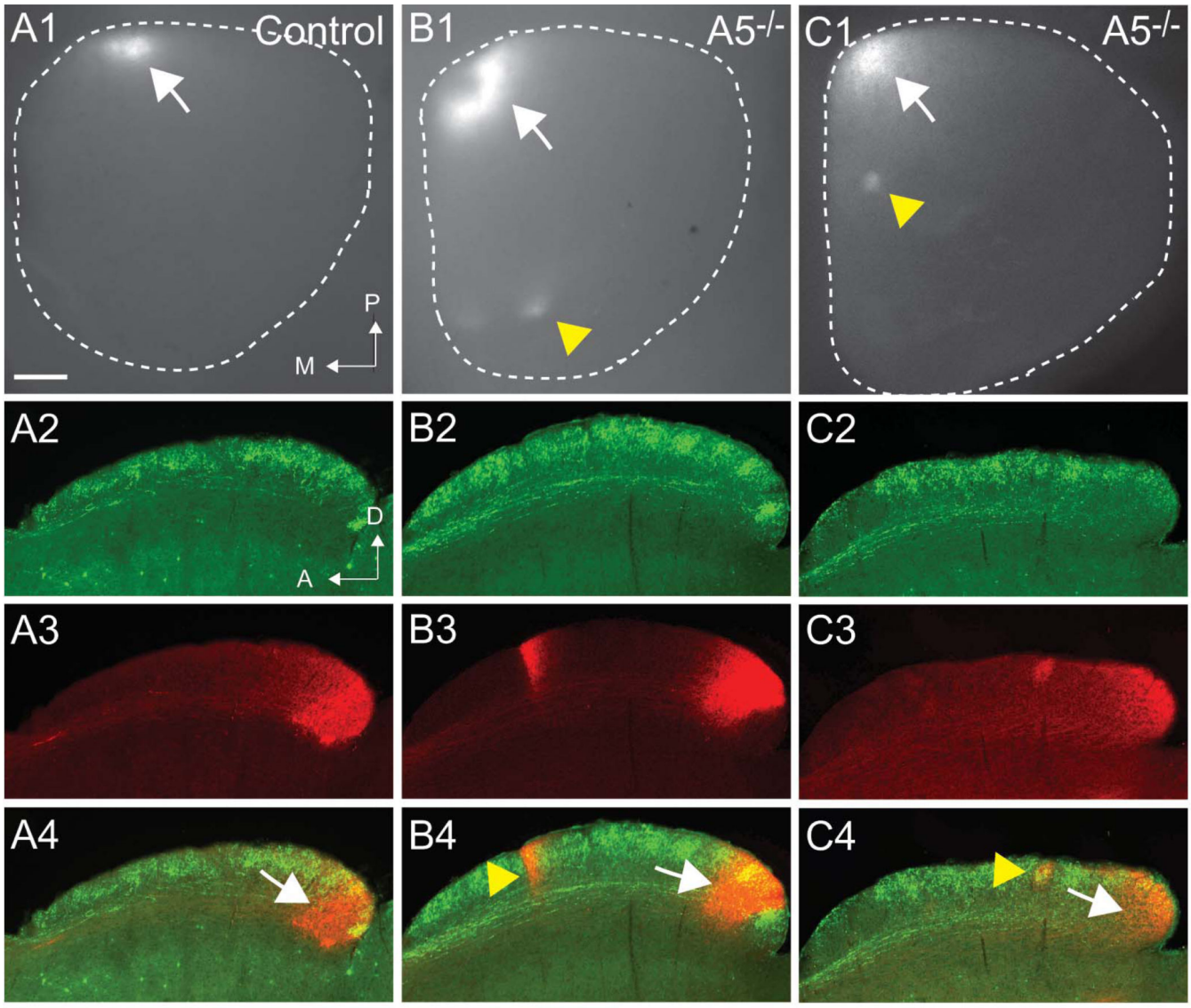

Figure 2. RGCs that project to topographically correct or incorrect locations in ephrin-A mutant mice do not belong to a specific RGC class

A1-C1. Whole mount images of superior colliculus with DiI-labeled RGCs from focal injections in the nasal retina in controls (A1) and ephrin-A5 mutant mice (B2, C2). Each shows a termination zone at the correct topographic location (white arrows), and ephrin-A5 mutants show ectopic termination zones at incorrect topographic locations (yellow arrowheads). White dotted lines show the dimensions of the SC; posterior is at the top, medial is to the left. A2-C4. Comparison TRHR-GFP RGCs that project to the superficial laminae (A2, B2, C2) with DiI-labeled RGCs (A3, B3, C3) show that ectopic TZs in ephrin-A5 mutants can project to all layers (B4, yellow arrowhead) or only to superficial laminae (C4, yellow arrowhead). A: anterior; D: dorsal; M: medial; P: posterior. Scale bar: 250 μm

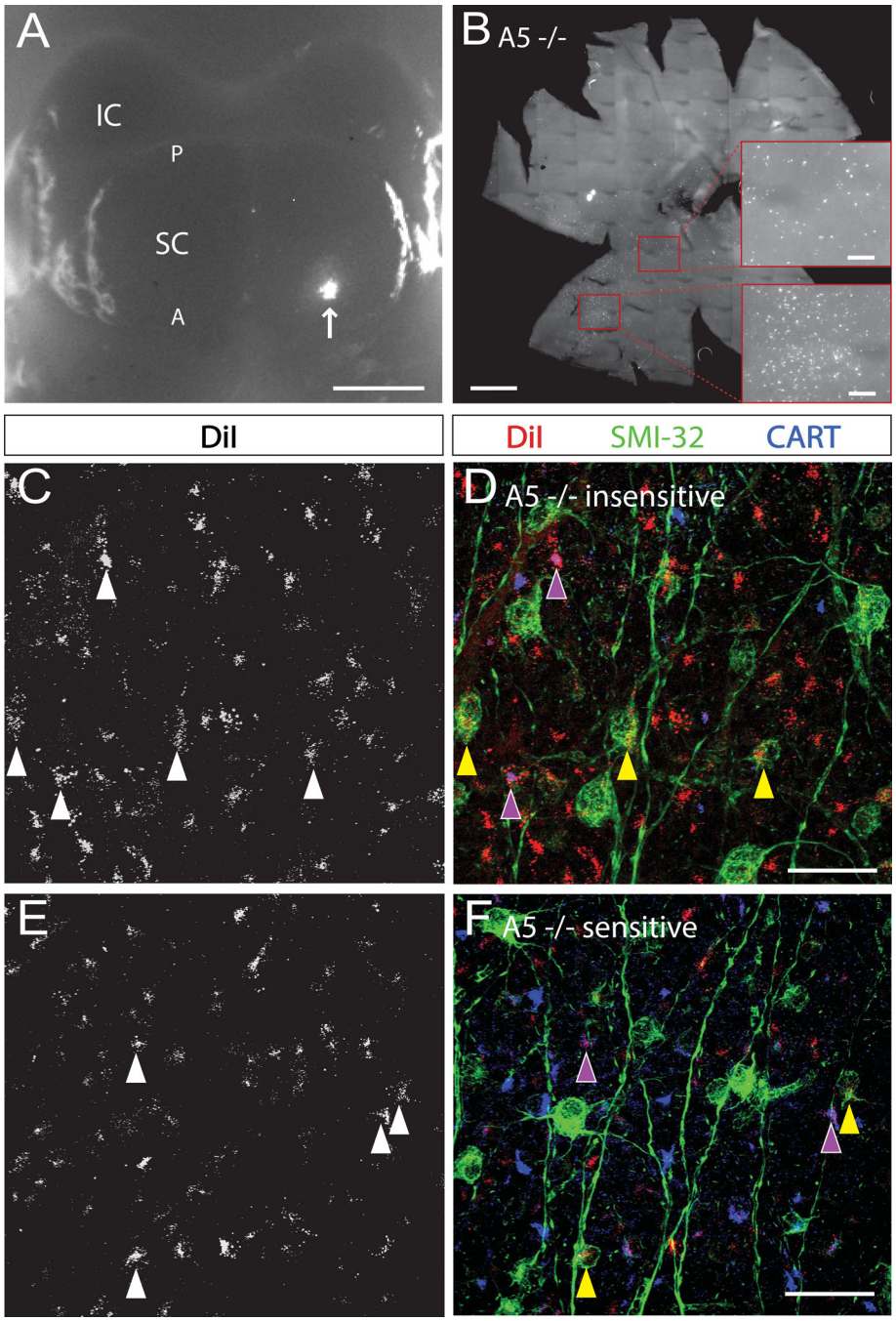

Figure 3. Different RGC types show different levels of dependence on ephrin-As in topographic mapping

A. Whole mount brain with unilateral DiI injection into superior colliculus indicated by arrow. IC, inferior colliculus; SC, superior colliculus; A, anterior; P, posterior. Scale bar, 1 mm. B. Flat-mounted retina (ganglion cell layer up) from an ephrin-A5 mutant mouse following injection of DiI into the contralateral superior colliculus. Scale bar, 500 μm. Bottom inset: topographically correct, A5−/− insensitive cluster of DiI+ cells. Top inset: topographically incorrect, A5−/− insensitive DiI+ cells. Scale bars, 100 μm. C, E. Maximal projections of A5−/− insensitive (C), and A5−/− sensitive (E), DiI+ RGCs, in an ephrin-A5

mutant mouse. D, F. Expression of CART or SMI-32 in a subset of the DiI-labeled cells shown in C and E, respectively. Arrowheads label single RGCs as follows: purple, CART +/DiI+; yellow, SMI32+/DiI+. Scale bars, 25 μm.

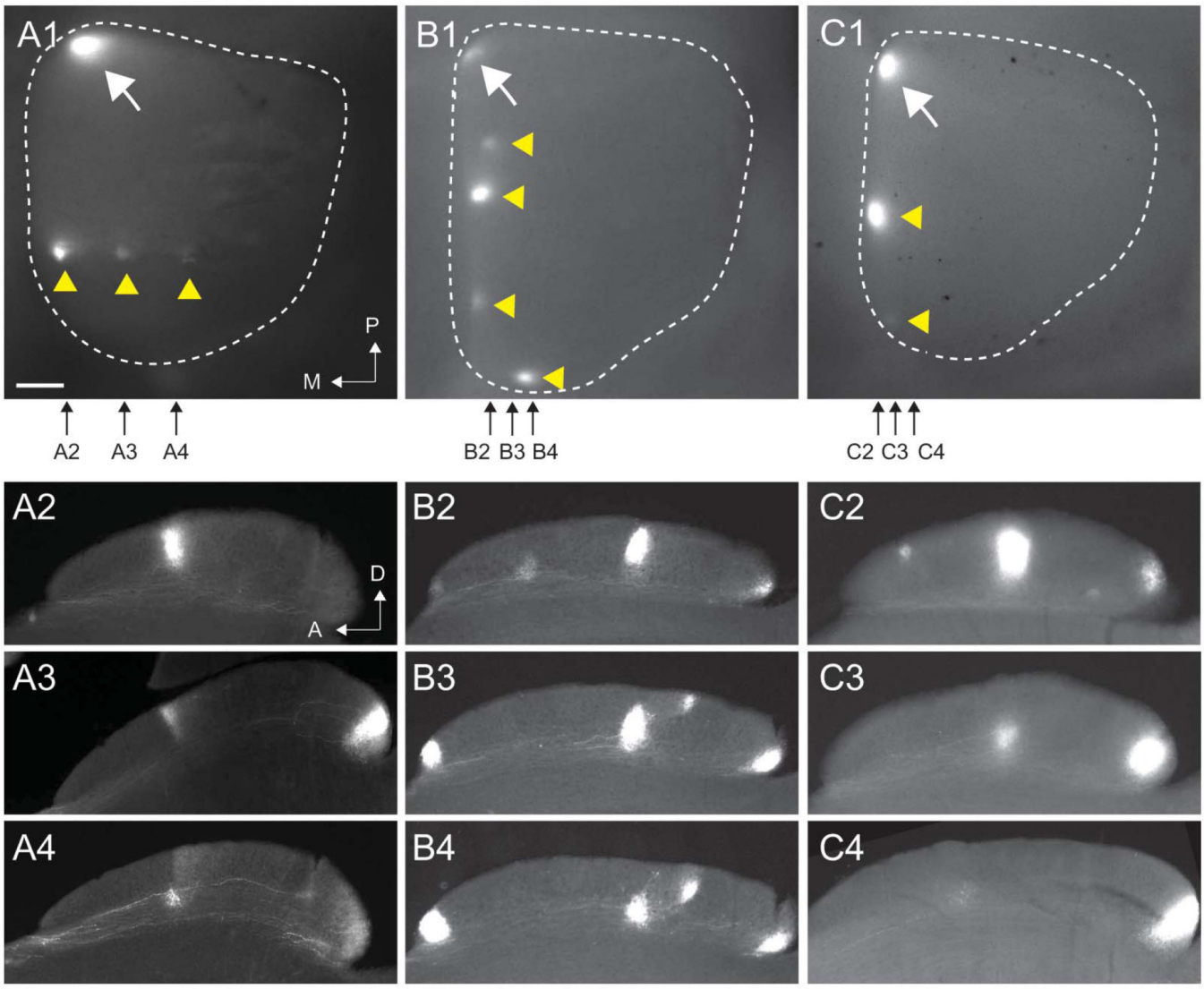

Figure 4. The topographic maps of different RGC types are misaligned in ephrin-A mutant mice

A1-C1. Three examples of whole mount images of superior colliculus showing DiI-labeled RGCs from focal injections in the nasal retina in ephrin-A2/A5 double knockouts. Each shows a termination zone at the correct topographic location (white arrows) and multiple ectopic termination zones at incorrect topographic locations (yellow arrowheads). White dotted lines show the dimensions of the SC; posterior is at the top, medial is to the left. Small black arrows show the approximate locations of the parasagittal sections shown in panels A2–A4, B2–B4 and C2–C4. A: anterior; D: dorsal; M: medial; P: posterior. Scale bar: 250 μm

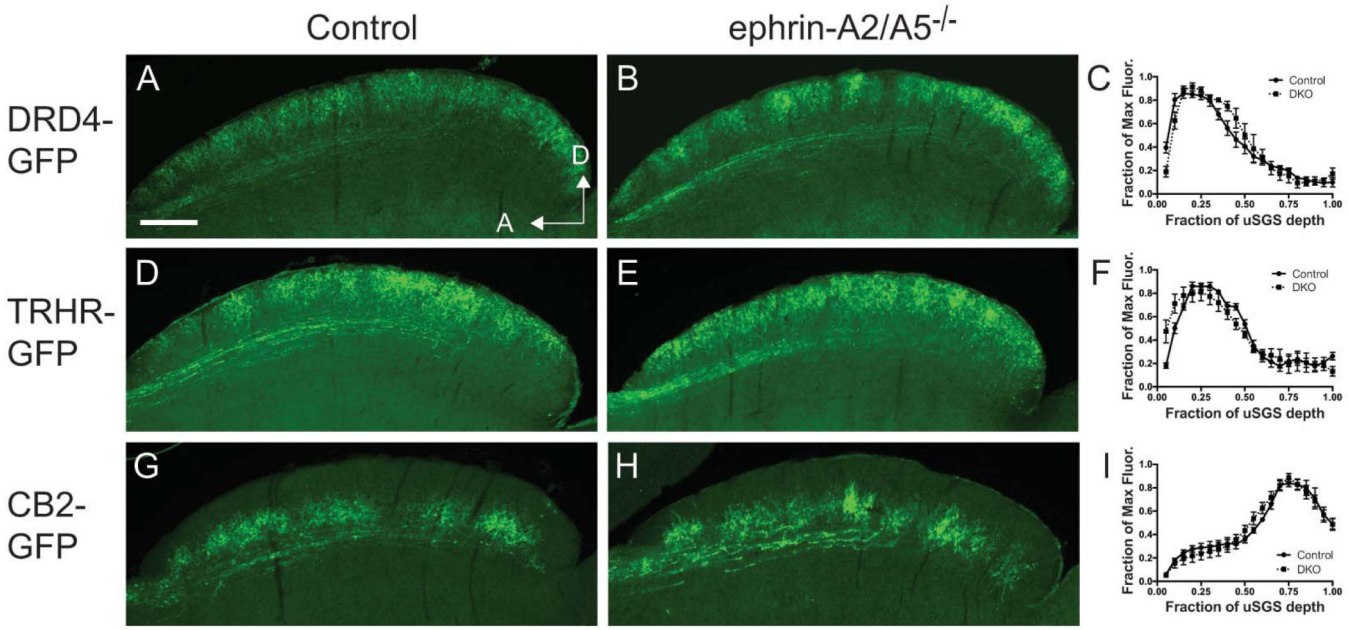

Figure 5. Lamination of RGC inputs is preserved in ephrin-A mutant mice

Parasagittal superior colliculus sections stained with anti-GFP antibody to visualize RGC axons labeled in DRD4-GFP (A–C), TRHR-GFP (D–F) and CB2-GFP (G–I) transgenic mouse lines. Quantification of GFP fluorescence across the RGC recipient layer of the SC (uSGS) is shown in the graphs in panels C, F and I. Scale bar: 250 μm

Table 1

Quantification of RGC types labeled via DiI injection into superior colliculus

The percentage of DiI-labeled cells of either type (SMI-32+ or CART+) is presented for ephrin-A5 insensitive (correctly targeted; top row) and ephrin-A5 sensitive (aberrantly targeted; bottom row) areas of the retinas of ephrin-A5 mutant mice. N (number of retinas examined) is indicated in parentheses for each set. The bottom row reports the results of Holm-Sidak's multiple comparison's test.

	SMI-32+/DiI+ as a % of DiI+ ±SEM	**Normalized SMI-32+/DiI+ asa % of DiI+ ±SEM**	**CART+/DiI+ asa % of DiI+ ±SEM**	**Normalized CART+/DiI+ asa % of DiI+ ±SEM**
Cluster (A5 insensitive)	**11.7**±3.2 (n=5)	**17.7**±2.7	**17.3**±2.1 (n=3)	**30.9**±7.6
Streak (A5 sensitive)	**16.2**±2.3 (n=5)	**28.9**±2.4	**5.7**±3.0 (n=4)	**19.3**±4.5
Significant diff?	-	No	-	No